

Temperature variability in X-ray bright points observed with Hinode/XRT

R. Kariyappa^{1,2}, E.E. DeLuca², S.H. Saar², L. Golub², L. Damé³, A.A. Pevtsov⁴, and
B.A. Vaghese¹

¹ Indian Institute of Astrophysics, Bangalore 560034, India

² Harvard-Smithsonian Center for Astrophysics, 60 Garden Street, Cambridge, MA, USA

³ Laboratoire Atmospheres, Milieux et Observations Spatiales (LATMOS), CNRS, BP 3, 91371
Verrières-le-Buisson Cedex, France

⁴ National Solar Observatory, PO Box 62, Sunspot, NM 88349, USA

Received / Accepted

ABSTRACT

Aims. Our aim is to investigate the variability in the temperature as a function of time among a sample of coronal X-ray bright points (XBPs).

Methods. We analysed a 7-hour (17:00 UT - 24:00 UT) long time sequence of soft X-ray images observed almost simultaneously in two filters (Ti_poly and Al_mesh) on April 14, 2007 with X-Ray Telescope (XRT) on-board the Hinode mission. We identified and selected a sample of 14 XBPs and 2 background coronal regions for a detailed analysis. The light curves of XBPs have been derived using SolarSoft library in IDL. The temperature of XBPs was determined using the calibrated temperature response curves of the two filters by intensity ratio method.

Results. We find that the XBPs show a high variability in their temperature and the average temperature ranges from 1.1 MK to 3.4 MK. The variations in the temperature are related to the different X-ray emission fluxes. These results suggest **that XBPs of different temperatures may be present** at the same height in the corona. It is evident from the results of time series that the heating rate of XBPs is highly variable on short time scales, and these variations provide a support for magnetic reconnection as the origin of XBPs.

Key words. Sun: corona – Sun: X-rays, gamma rays – Sun: magnetic topology

1. Introduction

Solar coronal X-ray bright points (XBPs) have been an enigma since their discovery in late 1960's (Vaiana et al. 1970). XBPs have been studied in great detail using Skylab and Yohkoh X-ray images (Golub et al. 1974; Harvey 1996; Nakakubo & Hara 1999; Longcope et al. 2001; Hara & Nakakubo 2003). Their correspondence with small bipolar magnetic regions was discovered by combining

Send offprint requests to: R. Kariyappa

ground-based magnetic field measurements with simultaneous space-borne X-ray imaging observations (Krieger et al. 1971; Golub et al. 1977). The number of XBPs (daily) found on the Sun varies from several hundreds up to a few thousands (Golub et al. 1974). Zhang et al. (2001) found a density of 800 XBPs for the entire solar surface at any given time. It is known that the observed XBP number is anti-correlated with the solar cycle, but this is an observational bias and the number density of XBPs is nearly independent of the 11-yr solar activity cycle (Nakakubo & Hara 1999; Sattarov et al. 2002; Hara & Nakakubo 2003). On the other hand, Sattarov et al (2010) found a modest decrease in number of coronal bright points in EIT/195 Å associated with the maximum of Cycle 23. Thus, the variation of the number of XBPs with solar cycle is still an open question.

Golub et al. (1974) found that the diameters of the XBPs are around 10-20 arc sec and their life time ranges from 2 hours to 2 days (Zhang et al. 2001, Kariyappa 2008). Studies have indicated the temperatures to be fairly low, $T = 2 \times 10^6$ K, and electron densities $n_e = 5 \times 10^9 \text{ cm}^{-3}$ (Golub & Pasachoff 1997), although cooler XBPs exist (Habbal 1990). XBPs are also useful as tracers of coronal rotation (Karachik et al 2006, Kariyappa 2008) and contribute to the solar X-ray irradiance variability (DeLuca and Saar 2009; Kariyappa & DeLuca 2009). Assuming that almost all XBPs represent new magnetic flux emerging at the solar surface, their overall contribution to the solar magnetic flux would exceed that of the active regions (Golub & Pasachoff 1997). Since a statistical interaction of the magnetic field is associated with the production of XBPs, the variation of the XBP number on the Sun will be a measure of the magnetic activity of its origin.

The chromospheric bright points are also observed using high resolution CaII H and K spectroheliograms and filtergrams. Extensive studies have been conducted to determine their dynamical evolution, the contribution to chromospheric oscillations and heating, and to UV irradiance variability (e.g. Liu 1974; Cram and Damé 1983; Kariyappa et al. 1994; Kariyappa 1994 & 1996; Kariyappa & Pap 1996; Kariyappa 1999; Kariyappa et al. 2005; Kariyappa and Damé 2010). The oscillations of the bright points at the higher chromosphere have been investigated using SOHO/SUMER Lyman series observations (Curdt & Heinzel 1998; Kariyappa et al. 2001). It is known from these studies that the chromospheric bright points are associated with 3-min periods in their intensity variations.

It has been investigated that the XBPs observed using Hinode/XRT and Yohkoh/SXT show an intensity oscillations on time scales of a few minutes to hours (Kariyappa and Varghese 2008 and Strong et al. 1992). Similar variations in brightness of coronal bright points observed with EIT data have been reported by Kankelborg and Longcope (1999). These oscillations may be indicative of impulsive energy released by small-scale reconnection events associated with BPs (Longcope and Kankelborg 1999). The X-ray Telescope on Hinode, XRT, has made long and continuous high temporal and spatial resolution time sequence observations of XBPs. In addition, the angular resolution of XRT is 1", which is almost three times better than that of Yohkoh/SXT instrument. Due to the wide coronal temperature coverage achieved with XRT observations, for the first time the XRT can provide complete dynamical evolution information for the XBPs. The study of the spatial and temporal relationship between the solar coronal XBPs and the photospheric and chromospheric magnetic features is an important issue in physics of the Sun. The Hinode/XRT observations provide an opportunity to investigate and understand more deeply the dynamical evolution and nature of the XBP than has been possible to date and to determine their relation to the large-scale magnetic

features. Such high resolution observations and investigations would be helpful in understanding the role of oscillations and the nature of the waves associated with XBPs to heat the corona.

The aim of this paper is to determine the temperature of XBPs using the soft X-ray images observed almost simultaneously in two filters and to show that both cooler and hotter XBPs are present in the corona.

2. Observations and analysis

The results presented in this paper are based on the analysis of a 7-hour (17:00 UT to 24:00 UT) time sequence of soft X-ray images obtained on April 14, 2007 almost simultaneously in Ti_poly & Al_mesh filters from XRT on-board Hinode (Golub et al., 2007). It is 2-min cadence images taken at the center of the solar disk in a quiet region. The image size is 512" x 512" in Ti_poly & 256" x 256" in Al_mesh. We have identified and selected 14 XBPs and 2 background coronal regions in both images. We have marked the 14 XBPs on both the images in Fig. 1 as xbp1, xbp2,....., xbp14 and 2 background coronal regions as xbp15 and xbp16. We used the routine `xrt_prep.pro` in IDL under SolarSoftWare (SSW) to calibrate the images including (i) removal of cosmic-ray hits and streaks (using the subroutine `xrt_clean_ro.pro`), (ii) calibration of read-out signals, (iii) removal of CCD bias, (iv) calibration for dark current, and (v) normalization of each image for exposure time. We have manually placed rectangular boxes covering the selected XBPs on the calibrated images and the box size will remain the same through out the time sequence. We checked by running the movie of the image sequence to make sure that the XBP is always within the box. A box serves as a proxy for XBP included in this box. Then we derived the cumulative intensity values of the XBPs by adding all the pixel intensity values inside corresponding boxes for the total duration of observations. The light curves of the XBPs have been derived from both the time sequence images.

Shortly after the launch of Hinode, the contamination from an unknown source began to deposit on the XRT CCD at a roughly constant rate. Routine CCD backouts do not completely remove this contamination. Although the actual substance(s) are not known, the optical properties, as judged by the change of the filter response to 'quiet Sun' plasma, are similar to diethylhexyl phthalate (DEHP). If modeled as DEHP, the contaminant layer at the time of our observations is estimated to be ≈ 1417 Å thick. The effect of the contaminant is highly wavelength dependent, with long wavelengths most absorbed. Consequently, the Al-mesh filter is much more affected than Ti_poly, although the effect in the latter is not negligible. XRT IDL software available in the SSW tree (`make_xrt_wave_resp.pro`, `make_xrt_temp_resp.pro`) was used to include this contamination layer in the filter temperature response for our analysis. After including the contamination layer we derived the filter response curves for both Ti_poly and Al_mesh filters. These curves are used to estimate the temperature of XBPs after determining the intensity ratios. To calculate temperature, Al_mesh images were interpolated to match Ti_poly image scale. Because both images were taken near-simultaneously, no sub-pixel co-alignment of images was performed. A more detailed discussion on data analysis is also presented along with the results in the following section.

3. Results and discussion

The temperature fluctuations and morphology of different X-ray bright points and associated plasma properties are not well understood. Some authors classified the bright points seen at dif-

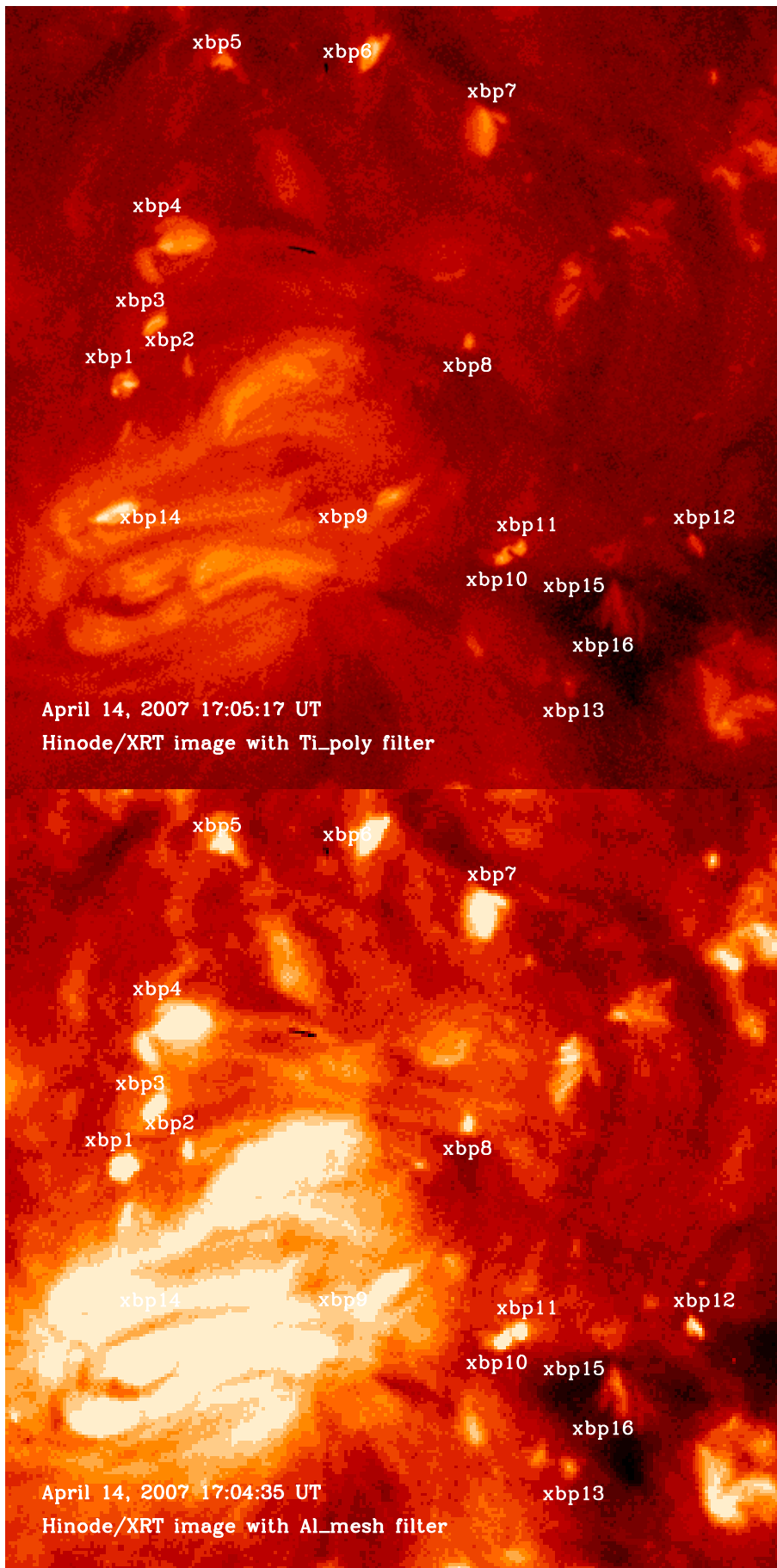


Fig. 1. Sample of X-ray images obtained on April 14, 2007 at the center of the solar disc in a quiet region in Ti_poly (*top panel*; 512'' x 512'') and Al_mesh (*bottom panel*; 256'' x 256'') filters with Hinode/XRT. The analysed XBPs are marked as xbp1, xbp2,.....xbp14 and the background coronal regions as xbp15 and xbp16.

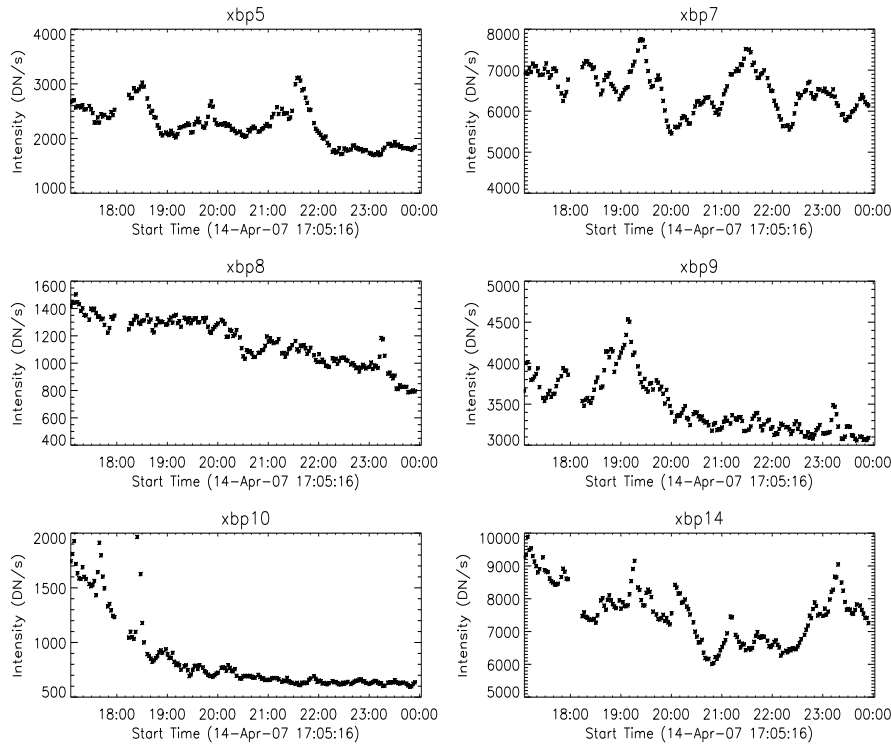


Fig. 2. Time series of XBPs (xbp5, xbp7, xbp8, xbp9, xbp10 & xbp14) observed in Ti_{poly} filter (intensity in DN/s versus start time).

ferent temperatures as the cool and hot components (McIntosh 2007; Tian et al. 2008) in transition region and corona respectively. It will be interesting to know whether there are cooler and hotter bright points (XBPs) at the coronal level.

Our Fig. 1 reveals the different types of XBPs showing different X-ray emission levels with a rich morphology. On the calibrated images we have placed rectangular boxes covering the selected XBPs and derived the cumulative intensity values of the XBPs by adding all the pixel intensity values. The light curves of all the XBPs have been derived for both the time sequence images. The light curves of 6 XBPs (e.g. xbp5, xbp7, xbp8, xbp9, xbp10 and xbp14) are shown in Fig. 2 for Ti_{poly} filter. Similarly in Fig. 3 we have shown the light curves of these XBPs observed with Al_{mesh} filter. The intensity oscillation is seen in all the light curves of the XBPs (presented in Figs. 2 and 3) observed with the two filters and the fluctuations are similar pattern in both cases. The temporal variations in the intensity of XBPs observed with Ti_{poly} filter show an intensity oscillations on time scales of a few minutes to hours (Kariyappa and Varghese 2008). From Figures 2 and 3 we notice that xbp8 do not show an impulsive brightness variations, instead the brightness is gradually decreasing. On the other hand, xbp5, xbp7, xbp9, xbp14 do show impulsive energy deposition presumably due to reconnection. Some of the variations in brightness shown on Figs. 2 and 3 could be the result of two effects: actual increase in surface brightness of XBP and increase in area of XBP. The latter effect can be mitigated by taking the ratio of images observed in two filters. We derived the ratio of the intensity values of each XBP observed with two filters. The variations of the intensity ratios are presented in Fig. 4 for xbp5, xbp7, xbp8, xbp9, xbp10 and xbp14. It is evident from these figures that the fluctuations in intensity ratio of XBPs are similar to the intensity oscillations as shown in Figs. 2 and 3.

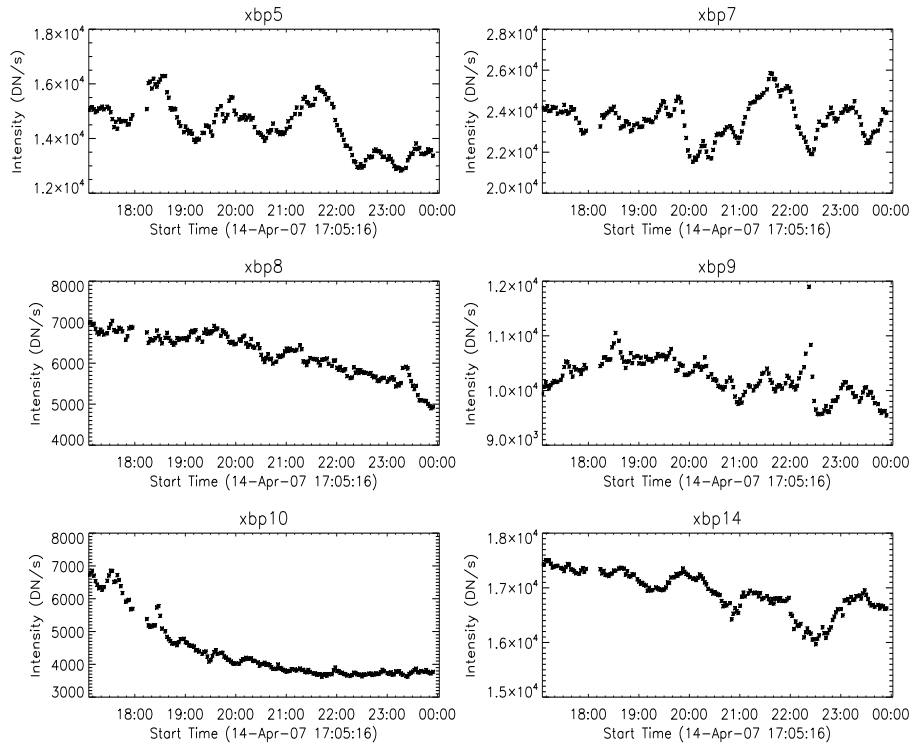


Fig. 3. Time series of XBPs (xbp5, xbp7, xbp8, xbp9, xbp10 & xbp14) observed in AL_mesh filter (intensity in DN/s versus start time).

Table 1. Mean temperature of XBPs

XBP	Temperature (MK)	XBP	Temperature (MK)
xbp1	1.30	xbp9	1.54
xbp2	1.24	xbp10	1.19
xbp3	2.31	xbp11	1.24
xbp4	1.24	xbp12	1.24
xbp5	1.11	xbp13	1.64
xbp6	1.23	xbp14	3.44
xbp7	1.18	xbp15	0.98
xbp8	1.53	xbp16	1.19

To determine the temperature of XBPs we derived the XRT filter temperature response curves for Ti_poly and AL_mesh after including the contamination layer (see Fig. 5). Using these filter temperature response curves and the intensity ratios we determined the temperature of each XBP. We estimated the errors in the temperatures by assuming photon statistics for the filter fluxes, and folding these through the filter ratio versus temperature to estimate temperature errors. We stress that these are random errors only; systematic errors due to uncertainties in, e.g., calibrations, the contamination layer, etc. are not included, but they are smaller than random errors. We estimate that the mean systematic errors in temperature estimation is of the order of ± 0.01 MK. For example in Fig. 6 we show the temporal variations in temperature of xbp5, xbp7, xbp8, xbp9, xbp10, & xbp14 with error bars (random errors).

All the XBPs show a temperature fluctuations similar to intensity oscillations although relationship between temperature and intensity oscillations is not linear (see Fig.7). We noticed that the

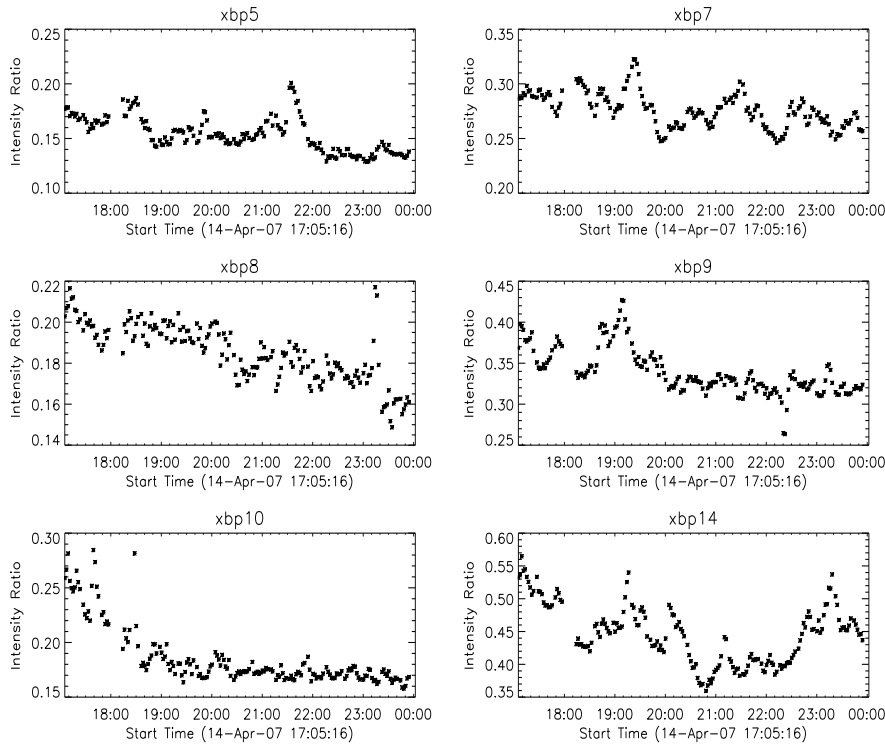


Fig. 4. Variation of intensity ratios (Ti_poly/Al_mesh) of XBPs: xbp5, xbp7, xbp8, xbp9, xbp10 & xbp14 (intensity ratio versus start time).

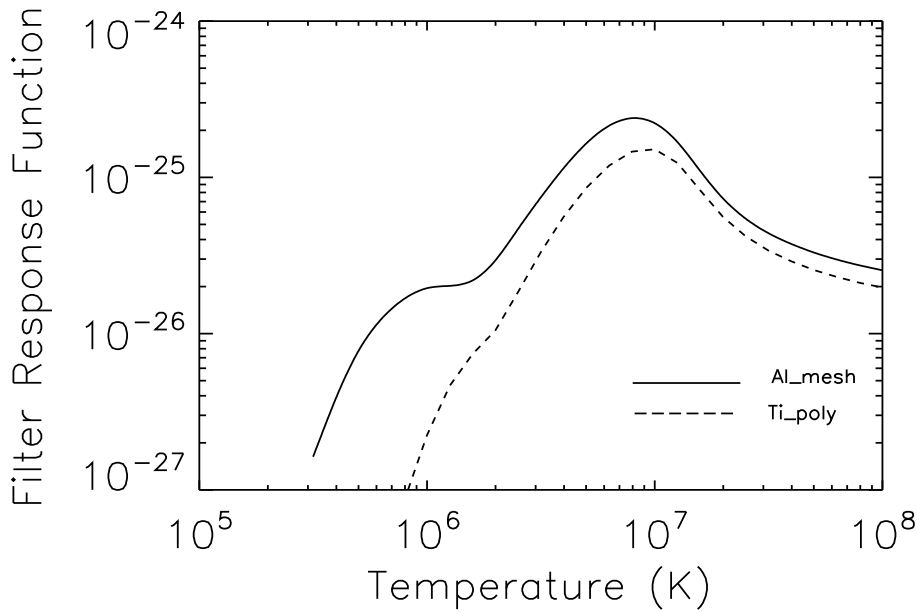


Fig. 5. Variations of XRT Ti_poly & Al_mesh filter responses as a function of temperature after including the contamination layer.

temperature is well correlated with the intensity of all the XBPs except in the case of xbp7 where the temperature is anti-correlated with the intensity. One possible explanation for the existence of anticorrelation in xbp7 could be that the xbp7 is at the end of the reconnection process, when the reconnection between two independent magnetic poles is nearly completed. Figure 3 (right panel) in Longcope and Kankelborg (1999) shows change in energy deposit as two poles approach and

reconnect with each other. The amount of energy increases, reaches a maximum, and decreases. So, xbp7 is at the late stages on that process, the reconnection episodes still continue, and they inject high temperature plasma into corona, but the amount of injected energy is relatively small as compared with the energy injected by previous episodes. So, there is a large amount of plasma that cools down due to radiative cooling; reconnection episodes still produce variation in brightness, but the high-temperature plasma (supplied by reconnection events) is masked by a bulk of cooler plasma already present above the reconnection site. We found a similar anticorrelation in xbp7 observed with Al_mesh filter. The above scenario, however, needs further verification via detailed study of evolution of magnetic properties of XBPs using high-cadence magnetograms. Unfortunately, no such magnetograms at sufficiently high cadence is available for time period described in this paper.

We noticed from the Fig. 6 and Table 1 that the average temperature of the 14 XBPs ranges from 1.1 MK to 3.4 MK. **The xbp14 is an interesting bright point located in an active region showing higher temperature value of 3.4 MK. This implies that xbp14 may be associated with different energization process in the presence of active region than in the rest of the XBPs. In addition we noticed in the light curve of xbp14 that there is sharp peak around 19:00 - 20:00 hours increasing the temperature to 7 MK (Fig.6) and this could be due to the occurrence of nanoflare. However we have only one such sample in our data set and it would be interesting to make a detailed study on a large sample of active region XBPs to understand the different processes and to compare with other XBPs. It is evident from the Fig.6 and Table I that the background coronal regions (xbp15 & xbp16) show much lower average temperature of 1.09 MK.** All XBPs (hot and cold) are observed in both filters. Temperature response curves for two filters have similar shape within 1 MK-100 MK range of temperatures, and Ti_poly filter has negligible contribution for plasma cooler than 1 MK. Thus, it is reasonable to assume that both filters sample same range of heights in solar corona. And latter can be interpreted as the presence of both cooler and hotter plasma in the corona through heights of XBP formation.

Whereas McIntosh (2007) classified the bright points seen in He II and soft X-ray as cool and hot bright points respectively. Similarly, Tian et al. (2008) show that the bright feature seen at coronal temperature as the hot component, and the corresponding bright emission at the transition region as the cool component of a bright point. These authors have examined the bright point observed at different heights in the solar atmosphere and hence they formed at different temperature levels, whereas we observed that **XBPs of different temperatures** are present at the same range of heights in the corona.

The use of filter ratios is only strictly valid for isothermal plasmas, and hence it is important to consider just how isothermal XBP plasma is. Brosius et al. (2008), using EUNIS on a sounding rocket, find a differential emission measure (DEM) peak at $\log T \sim 6.15$ and a minimum at $\log T \sim 5.35$ a factor of 3.5 lower in DEM. A similar peak temperature was found earlier by Habbal et al. (1990). Tian et al. (2008) note a two component structure, one at $\log T \approx 6.1 - 6.3$ and one at transition region temperatures $\log T \approx 5.2 - 5.4$ (see also McIntosh 2007). XRT is progressively less sensitive to plasma below $\log T \approx 6.0$ (Fig. 5), and so primarily sees the narrow hot component; Saar et al (2009) saw slightly varying $\langle \log T \rangle$ in a narrow peak around $\log T \sim 6.1$. Thus, while the DEM may not fall off enormously for $\log T < 6.0$ (Brosius et al 2008), the drop-off in XRT sensitivity may be sufficient to effectively isolate the hotter XBP DEM peak and that XBPs may be *effectively* isothermal for XRT purposes.

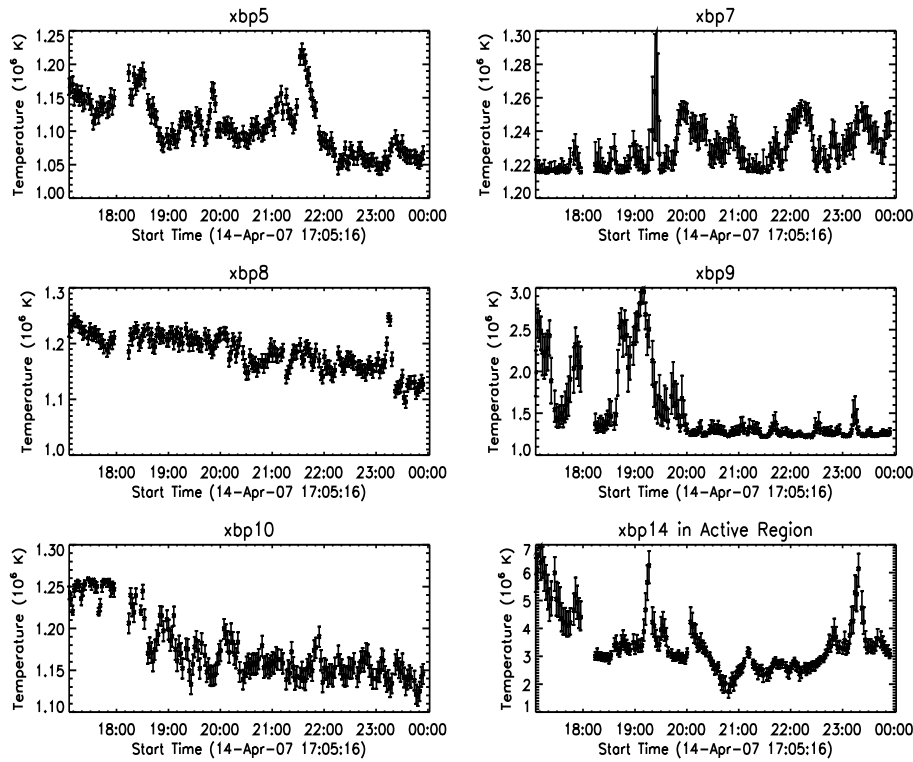


Fig. 6. Temperature variations in xbp5, xbp7, xbp8, xbp9, xbp10, & xbp14. The error bars are shown and the mean error in the estimated temperature is about ± 0.01 MK. (temperature in MK versus start time)

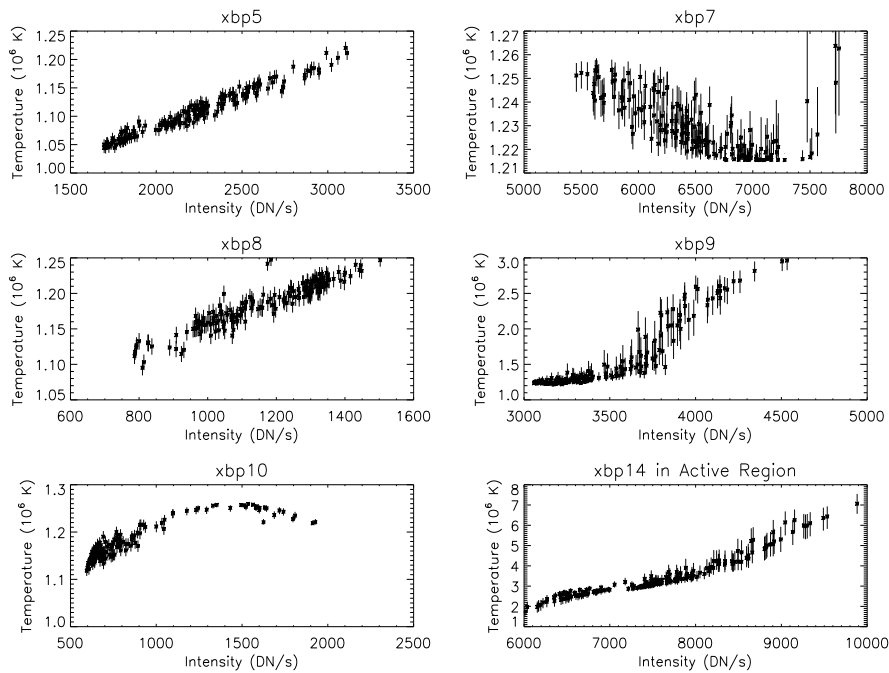


Fig. 7. Scatter diagrams of intensity in Ti_poly versus the temperature of XBPs (xbp5, xbp7, xbp8, xbp9, xbp10, & xbp14). (intensity in DN/s versus temperature in MK)

It is interesting to know how the temperature of XBPs (both cooler & hotter) are related with the strength of the magnetic field and how the magnetic field play a role in driving the different brightenings and different temperature values and in the heating mechanisms of the corona at the sites of XBPs. This would require a detail investigation of high resolution and high-time cadence

magnetograms, which were not available for a given sequence of XRT observations. Still, one can get useful insights from the dynamical evolution and changes in the morphology of XBPs. Our analysis of long time series observational data taken in multiple filters of the XBPs reveal more of the dynamical nature and the physical properties of different classes (cooler & hotter) of XBPs. **XBPs exhibit a temperature fluctuations in time (Fig.6) and the mean temperatures in the range of 1.1 MK to 3.4 MK suggesting for the presence of both colder and hotter plasma at the same height in the corona.** We speculate that the temperature fluctuations may be associated with reconnection of magnetic field forming XBPs. Comparing Figures 2, 3 and 6, we see that some XBPs (e.g., xbp8) do not show an impulsive variations, but both brightness and temperature are gradually decreasing. This indicates that in the case of xbp8 the reconnection process is completed, and what we see is plasma slowly cooling down. However, the radiative cooling time in the corona should be about 5-20 minutes (e.g., Aschwanden, 2004), and so, it could be that the reconnection still takes place, but there is no impulsive reconnection. On the other hand, xbp5, xbp7, xbp9, xbp14, and may be xbp10 do show impulsive energy deposition due to reconnection and the high temperature plasma in these cases is an indicative of the reconnection. The temperature values and their variations suggest that the XBPs show a high variability in their temperature and the heating rate of XBPs is highly variable on short time scales. To verify the above evolution requires detail study of thermal and magnetic properties of XBPs, which we plan to conduct in near future.

Acknowledgements. Hinode is a Japanese mission developed and launched by ISAS/JAXA, collaborating with NAOJ as a domestic partner, NASA and STFC (UK) as international partners. Scientific operation of the Hinode mission is conducted by the Hinode science team organized at ISAS/JAXA. This team mainly consists of scientists from institutes in the partner countries. Support for the post-launch operation is provided by JAXA and NAOJ (Japan), STFC (U.K.), NASA (U.S.A.), ESA, and NSC (Norway). We are grateful to the Hinode team for all their efforts in the design, build, and operation of the mission. The authors would like to thank Professor Loren Acton for stimulating discussion and valuable suggestions on this research. One of the authors (Kariyappa) wish to express his sincere thanks to Professor Siraj Hasan, Director, Indian Institute of Astrophysics for constant support & encouragement provided during this research work. The National Solar Observatory (NSO) is operated by the Association for Research in Astronomy (AURA, Inc.) under cooperative agreement with the National Science Foundation (NSF). We wish to express our sincere thanks to referee for valuable comments and suggestions that improved the manuscript considerably.

References

- Aschwanden, M. 2004, *Physics of the Solar Corona*, Springer-Praxis
- Brosius, J.W., Rabin, D.M., Thomas, R.J., & Landi, E. 2008, *ApJ*, 677, 781
- Cram, L. E., & Damé, L. 1983, *ApJ*, 272, 355
- Curdt, W., & Heinzel, P. 1998, *ApJ*, 503, L95
- DeLuca, E. E. & Saar, S.H. 2009, in preparation
- Golub, L., Krieger, A.S., Silk, J.K., Timothy, A.F., & Vaiana, G.S. 1974, *ApJL*, 189, L93
- Golub, L., Krieger, A.S., Harvey, J.W., & Vaiana, G.S. 1977, *Sol. Phys.*, 53, 311
- Golub, L., & Pasachoff, J.M. 1997, *The Solar Corona*, Cambridge University Press, Cambridge, United Kingdom.
- Golub, L., DeLuca, E., Austin, G., Bookbinder, J., Caldwell, D., Cheimets, P., Cirtain, J., Cosmo, M., Reid, P., Sette, A., Weber, M., Sakao, T., Kano, R., Shibasaki, K., Hara, H., Tsuneta, S., Kumagai, K., Tamura, T., Shimojo, M., McCracken, J., Carpenter, J., Haight, H., Siler, R., Wright, E., Tucker, J., Rutledge, H., Barbera, M., Peres, G., and Varisco, S. 2007, *Sol. Phys.*, 243, 63
- Habbal, S.R. 1990, in *Mechanisms of Chromospheric and Coronal Heating*, eds. P. Ulmschneider, E.R. Priest, and R. Rosner, Springer Verlag 127
- Habbal, S.R., Withbroe, G.L., & Dowdy, J.F. Jr. 1990, *ApJ*, 352, 333
- Hara, H., & Nakakubo-Morimoto, K. 2003, *ApJ*, 589, 1062

- Harvey, K.L. 1996, in *Magnetic Reconnection in the Solar Atmosphere*, eds. R. D. Bentley and J.T. Mariska, ASP Conf. Ser., 111, 9
- Kankelborg, C.C. & Longcope, D.W. 1999, *Sol. Phys.*, 190, 59
- Karachik, N. V., Pevtsov, A.A., & Sattarov, I. 2006, *ApJ*, 642, 562
- Kariyappa, R. 1994, *Sol. Phys.*, 154, 19
- Kariyappa, R. 1996, *Sol. Phys.*, 165, 211
- Kariyappa, R. 1999, in *19th NSO/Sac Peak Summer Workshop on High Resolution Solar Physics: Theory, Observations, and Techniques*, ASP Conf. Ser., 183, 420
- Kariyappa, R., & Pap, J. M. 1996, *Sol. Phys.*, 167, 115
- Kariyappa, R., Sivaraman, K. R., & Anandaram, M. N. 1994, *Sol. Phys.*, 151, 243
- Kariyappa, R., Varghese, B.A., & Curdt, W. 2001, *A & A.*, 374, 691
- Kariyappa, R., Satyanarayanan, A., & Damé, L. 2005, *Bull. Astron. Soc. India*, 33, 19
- Kariyappa, R., & Varghese, B.A. 2008, *A & A.*, 485, 289
- Kariyappa, R. 2008, *A & A.*, 488, 297
- Kariyappa, R., & DeLuca, E. E. 2009, in preparation
- Kariyappa, R., & Damé, L. 2010, *Sol. Phys.*, under review
- Krieger, A.S., Vaiana, G.S., & Van Speybroeck, L. P. 1971, in *Solar Magnetic Fields*, ed. R. Howard, IAU Symp. 43, 397
- Longcope, D.W. & Kankelborg, C.C. 1999, *ApJ*, 524, 483
- Liu, S. Y. 1974, *ApJ*, 189, 359
- Longcope, D.W., Kankelborg, C.C., Nelson, J. L., & Pevtsov, A. A. 2001, *ApJ*, 553, 429
- McIntosh, S.W. 2007, *ApJ*, 670, 1401
- Nakakubo, K., & Hara, H. 1999, *Adv. Space Res.*, 25(9), 1905
- Saar, S. H., Farid, S. & DeLuca, E.E. 2009, in *American Institute of Physics Conference Series (AIPC)*, 1094, 756
- Sattarov, I., Pevtsov, A.A., Karachik, N. V., Sherdanov, C.T. & Tillaboev, A.M. 2010, *Sol. Phys.*, 262, 321
- Sattarov, I., Pevtsov, A.A., Hojaev, A.S., & Sherdonov, C.T. 2002, *ApJ*, 564, 1042
- Strong, K.T., Harvey, K., Hirayama, T., Nitta, N., Shimizu, T., & Tsuneta, S. 1992, *PASJ*, 44, L161
- Tian, H., Curdt, W., Marsch, E. & He, J.-S. 2008, *ApJ*, 681, L121
- Ugrte-Urra, I., Doyle, J.G., Madjarska, M.S., & O'Shea, E. 2004, *A & A.*, 418, 313
- Vaiana, G.S., Krieger, A.S., Van Speybroeck, L.P., & Zehnfennig, T. 1970, *Bull. Am. Phys. Soc.*, 15, 611
- Zhang, J., Kundu, M., & White, S. M. 2001, *Sol. Phys.*, 88, 337